

# Visualization Methods of Vortex Structures Acting on the Wing in High-Speed Flows

T.V. Konstantinovskaya<sup>1,A</sup>, V.E. Borisov<sup>2,A</sup>, A.E. Lutsky<sup>3,A</sup>

Keldysh Institute of Applied Mathematics RAS

<sup>1</sup> ORCID: 0000-0002-1127-503X, [konstantinovskaya.t.v@gmail.com](mailto:konstantinovskaya.t.v@gmail.com)

<sup>2</sup> ORCID: 0000-0003-4448-7474, [narelen@gmail.com](mailto:narelen@gmail.com)

<sup>3</sup> ORCID: 0000-0002-4442-0571, [allutsky@yandex.ru](mailto:allutsky@yandex.ru)

## **Abstract**

This paper considers the use of vortex structures scientific identification and visualization methods in analyzing the effects of these structures on the wing at an angle of attack in supersonic flows. The results of applying the methods of scientific identification and visualization of vortex flows for the analysis and processing of numerical data of supersonic flow are presented. In the considered problem, the generator wing and the main wing are located at an angle of attack of 20° degrees to the incoming flow. Two configurations with different length of the vortex generator are considered. The simulation was carried out using URANS equations. Numerical simulations were performed on the hybrid supercomputer system K-60 at the Keldysh Institute of Applied Mathematics of the Russian Academy of Sciences. The scientific visualization of the simulation results was carried out primarily using the Liutex vortex structures identification criterion, which belongs to the third generation of such methods. And this method was effectively complemented and enhanced by the use of other methods.

**Keywords:** Supersonic flow visualization, tip vortex, vortex structures identification, vortex surface interaction.

## **1. Introduction**

In the modern world, movement speeds are of great importance and have a decisive role in choosing a means of transportation. Moreover, this issue is important for all spheres of human activity: both for leisure and for all types of industry. In this connection, attention is again increasing to the development of high-speed aircraft in various fields of application.

A detailed study of the aerodynamics of high-speed aircraft flight plays an important role in their development and construction. One of the important tasks is to study the influence of vortex structures on the aerodynamics of aircraft, since the formation of vortex structures accompanies the flight of any aircraft. In particular, the importance of research and development on the tip vortices interaction in high-speed flows is vital for several reasons:

- safety: effective vortex prediction and management is essential to prevent catastrophic failures during flight.
- performance: understanding the effects of vortex structures can lead to improved aerodynamic designs, enhancing payload delivery and overall mission success.
- innovation: ongoing research leads to the discovery of new forms and methods that can revolutionize the aerospace industry, enabling new missions and capabilities.

The study of the interaction of vortex structures with the aircraft surface is of particular interest, most notably, interaction of such structure as a tip vortex. A tip vortex forms on the wings or on other finned parts of bodies as a result of the pressure difference between the upper and lower surfaces.

Special methods of scientific identification and visualization of vortex structures can be effectively used for processing and analyzing the results of numerical and experimental modeling, providing tools not only for visualization of flows, but also for their analysis [1-4]. In particular, they can highlight the position of the main vortex structures.

With the development of numerical methods and the growth of the volume of processed data, the development of vortex structures identification scientific methods does not lose relevance and many researchers are interested in this topic. That is evidenced by the ongoing relevant work and the involvement of new methods and approaches to the problems of identification and visualization of vortex structures (e.g. [5-8]).

In this paper, the problem of identification and visualization of vortex structures is considered by the example of application to the results obtained in the numerical study of the effect of vortex structures on the wing in supersonic mode. Using the methods of scientific identification of vortex structures, the effect of the tip vortex and the vortex sheet from the upward vortex generator on the flow around the main wing is shown. Two configurations are considered, differing in the length of the vortex generator. For visualization, the Liutex criterion for the identification of vortex flows is mainly used [9-15]. The Liutex criterion has also been complemented by other methods and the advantage of using various methods of this kind together has been demonstrated. The URANS approach with the SA turbulence model was used for the simulations. Simulations were carried out on the multiprocessor hybrid system K-60 at the Keldysh Institute of Applied Mathematics of the Russian Academy of Sciences.

## 2. Problem statement

This paper presents the results obtained in the study of supersonic flow around two wings arranged sequentially one after the other in the direction of the freestream with the Mach number of the incoming flow  $M_\infty = 3$ . The wings were rectangular in plan with sharp front, side and trailing edges. The half-span of the main wing was  $l_1 = 0.095$  m, the front vortex generator was  $l_2 = 0.0475$  m in the first configuration (short generator), in the second –  $l_2 = 0.095$  m (long generator), the chord of both wings was  $b = 0.03$  m. The distance between the axes of the wings was 4 chords in the direction of flow. The axis of the main wing was located behind the trailing edge of the front wing (generator) downstream in the direction of flow. The angle of attack of the wings was  $20^\circ$ , the Mach number of the incoming flow was  $M_\infty = 3$ , the Reynolds number was set  $Re_L = 1 \times 10^7$  ( $L$  is the characteristic length of the dimensionalization of the computational model, here  $L = 1$  m). Figure 1 shows a scheme of the computational domain.

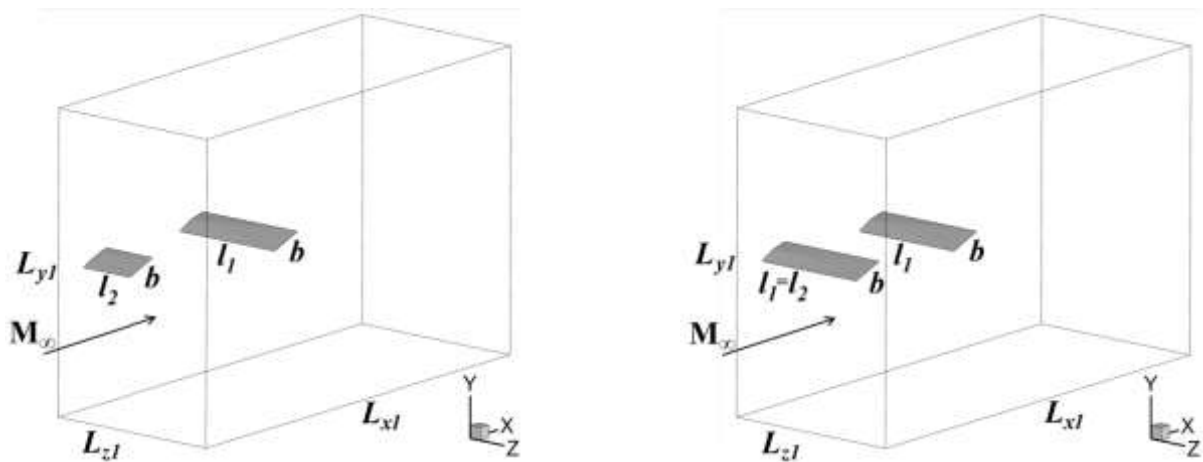


**Figure 1:** Computational domain, wings installation

The flow was considered at a distance of up to 6.5 wing chords downstream from the trailing edge of the main wing.

Here and further in the text of the article, configuration 1 refers to the flow option with a short generator, configuration 2 – with a long generator.

### **3. Numerical algorithm**

Simulations of the three-dimensional turbulent flow of a compressible gas were carried out using a system of unsteady Reynolds and Favre averaged Navier-Stokes equations (URANS). The Spalart-Allmaras (SA) one-parameter turbulence model was used to determine the value of turbulent viscosity. Its modification for compressible flows [16] was applied. The initial and boundary conditions were set in a standard way.

The approximation of the model equations was carried out in space using the finite volume method with a TVD reconstruction scheme of the 2nd order of accuracy. The finite volume method, assuming that the computational domain is covered by a grid consisting of non-overlapping polyhedral cells, is implemented by integrating a system of model equations for each counting cell, followed by converting volumetric integrals from flows into surface integrals along the cell faces. The generalized S. K. Godunov method with an exact Riemann solver was used to calculate inviscid flows on the faces of the calculated cells [17]. Both explicit and implicit (based on the LU-SGS method) schemes were used to approximate the equations in time. The used numerical method is described in [18].

The author's software package ARES was used to perform numerical simulations [19]. The simulations were carried out on the hybrid supercomputer system K-60 [20]. Unstructured grids containing about 5 million hexagonal cells were used for each of the configurations for presented task.

### **4. Visualization of flow vortex structures**

A special post-processing module has been developed as a part of the author's software package ARES, which allows to identify and analyze vortex structures on hexagonal grids. Within its framework, some methods of scientific identification and visualization of vortex structures have been implemented. Among them there are classical methods of scientific visualization, such as  $\lambda_2$ ,  $Q$ -criterion, etc. [21 - 23]. In addition, the module also contains the Liutex method of scientific visualization, one of the most modern criteria for the identification of vortex structures, belonging to the third generation of such methods.

This post-processing module generates output data in the format of the Tecplot software package.

This paper presents the results of numerical simulations and their visualization obtained using methods of vortex structures identification and visualization, mainly using the Liutex criterion. As the practice of its application by the authors shows, for a number of tasks it allows to obtain significantly more accurate results [24] in comparison with results of classical methods application. Which is quite understandable, taking into account the peculiarities of Liutex criterion construction. We shall describe them below. Descriptions of other methods for identifying vortex structures may be found in the literature (e.g. [21 - 23]).

#### **4.1. Liutex visualization method**

The Liutex method (or criterion) for the identification and visualization of vortex structures is one of the most modern, it belongs to the so-called third generation of such criteria. This criterion is free from the shear and compressive components of the strain rate tensor by its construction [9], which reduces the possibility of misdefinition of vortex structures by this criterion. The Liutex criterion allows you to evaluate the direction as well as the strength of vortices.

The criterion was proposed in 2018 under the name Rortex criterion [10], subsequently it was renamed as Liutex after one of the authors [11].

According to this criterion, the flow region with vortex structures is considered to be one in which the strain rate tensor has one real  $\lambda_r$  and two complex conjugate eigenvalues  $\lambda_{cr} \pm \lambda_{ci}$ . Using these eigenvalues, the Rortex vector [12] is determined, which locally coincides with the axis of rotation of the vortex as a solid body:

$$\mathbf{R} = \mathcal{R} \mathbf{r}, \quad \mathcal{R} = \boldsymbol{\omega} \cdot \mathbf{r} - \sqrt{(\boldsymbol{\omega} \cdot \mathbf{r})^2 - 4\lambda_{ci}^2},$$

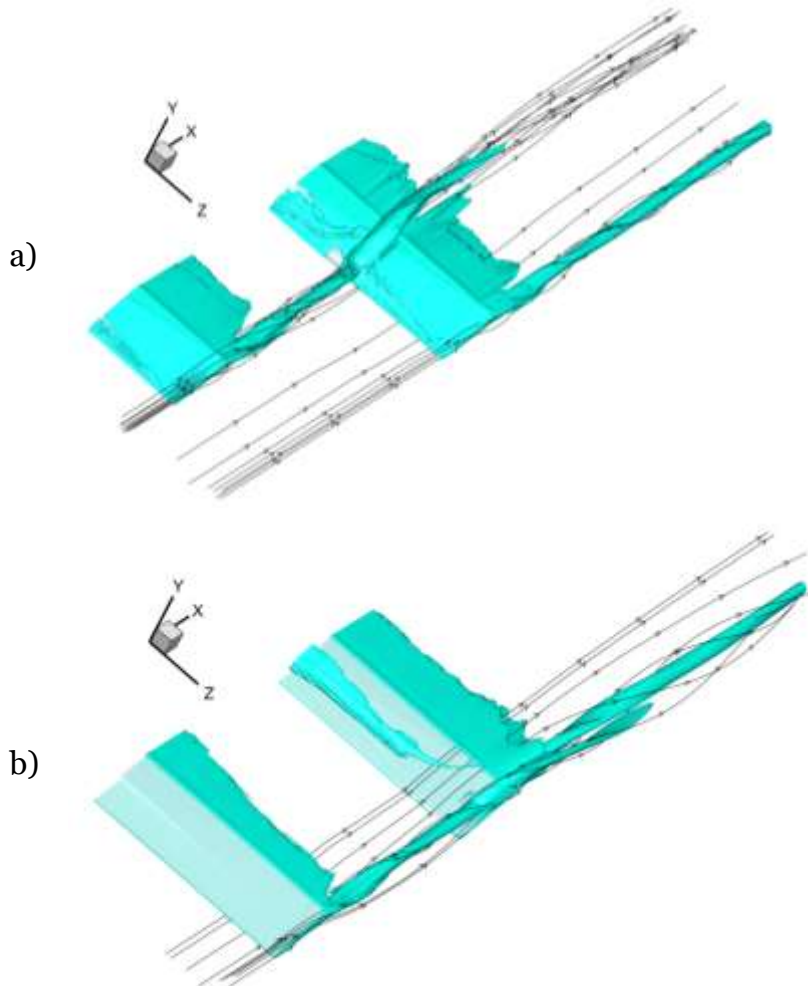
where  $\boldsymbol{\omega}$  – is the local vorticity vector,  $\mathbf{r}$  – normalized eigenvector corresponding to  $\lambda_r$  with condition  $\boldsymbol{\omega} \cdot \mathbf{r} > 0$ . On its basis, a normalized value  $\tilde{\Omega}_R \in [0, 1]$  is formed, showing the flow local rotation intensity:

$$\tilde{\Omega}_R = \frac{(\boldsymbol{\omega} \cdot \mathbf{r})^2}{2 \left[ (\boldsymbol{\omega} \cdot \mathbf{r})^2 - 2\lambda_{ci}^2 + 2\lambda_{cr}^2 + \lambda_r^2 \right] + \varepsilon_{Lu}}, \quad \varepsilon_{Lu} = k \max\{\lambda_{ci}^2\}.$$

Where  $\varepsilon_{Lu}$  – value dedicate to numerical “noise” filtration, maximum  $\lambda_{ci}$  is on all considered domain,  $k = 0.001 \sim 0.002$  [12].

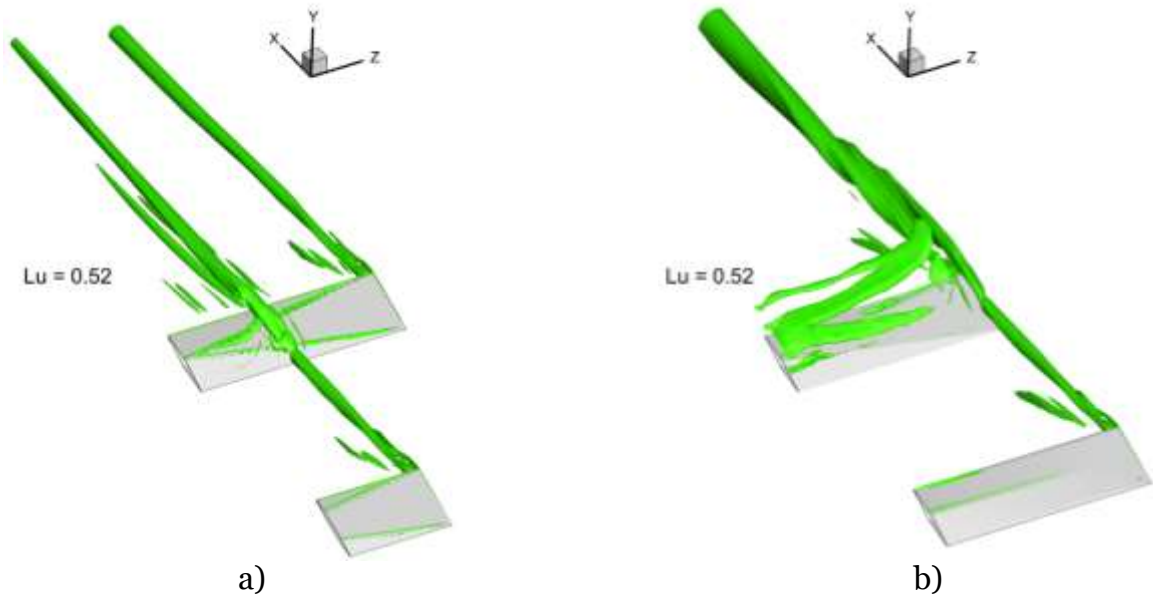
## 5. Simulation results and their visualization

Figure 2 shows a general view of the resulting flow for both configurations considered, a) for a short generator, b) for a long one.



**Figure 2:** General view of obtained flows in the considered configurations

In Figure 2 the flow results are visualized by means of streamlines and vorticity isosurfaces  $Vort$  (vorticity value 350), i.e. in other words, the results of using the vorticity method for identification and visualization of vortex structures are shown here [25]. In this visualization, two main components of the vortex wake behind the wing are clearly distinguishable – a vortex sheet and a tip vortex with a clearly distinguishable longitudinal structure. However, details of the flow are not visible, such as, for example, secondary vortices that arise when the generator tip vortex interacts with the main wing surface.



**Figure 3:** Visualization of vortex structures using the Liutex criterion: isosurface  $\tilde{\Omega}_R = 0.52$ , for configurations with a short generator (a) and a long one (b)

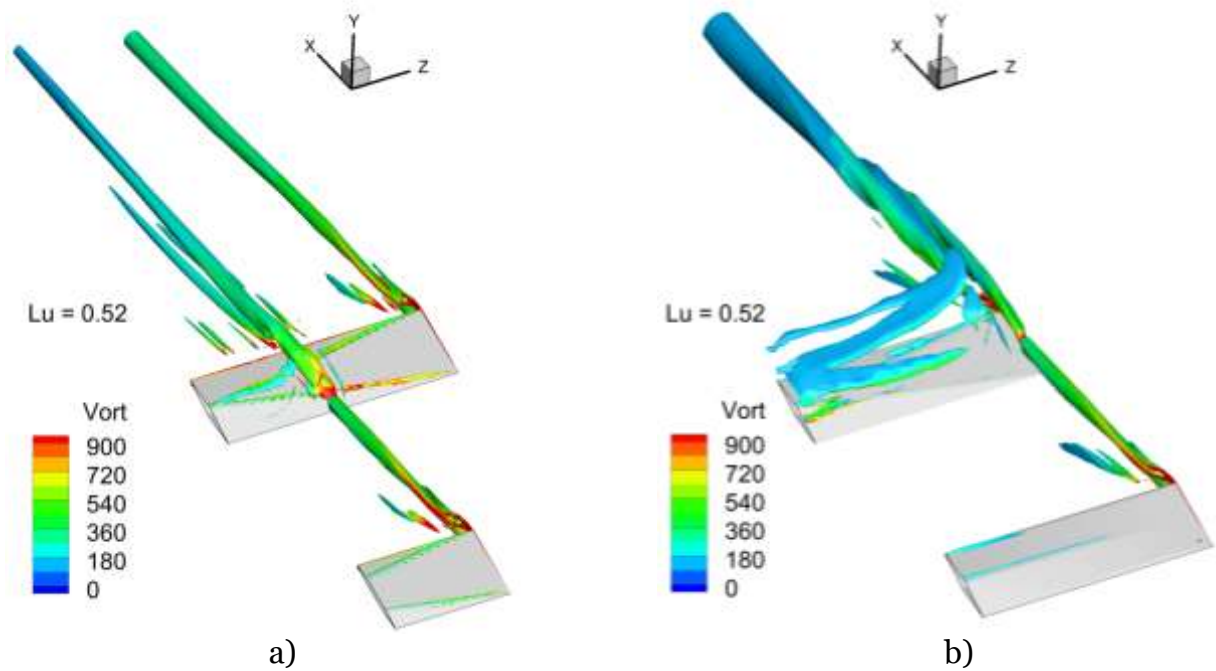


**Figure 4:** Visualization of vortex structures using both the Liutex criterion and the vorticity: isosurface  $\tilde{\Omega}_R = 0.52$  with values of vorticity ( $Vort$ ) on it, for configurations with a short generator (a) and a long one (b)



Figure 3 shows the visualization of the flow using the Liutex criterion for the vortex structures identification for the considered configurations with a short (a) and a long (b) generator. To display the Liutex isosurface, the standard value of the parameter  $\tilde{\Omega}_R = 0.52$  is used, which is sufficient to determine the main vortex structures for such flows.

The resulting visualization of vortex structures is quite homogeneous and featureless, and more clarity can be added to it by additionally displaying the vorticity values (*Vort*) on the isosurface of the Liutex criterion. In Figures 4 – 6 the considered flows are visualized with simultaneous use of the Liutex criterion and the vorticity method, which gives a more visual representation of the vortex intensity, which is greater right behind a wing and decreases as it moves downstream from the wing.

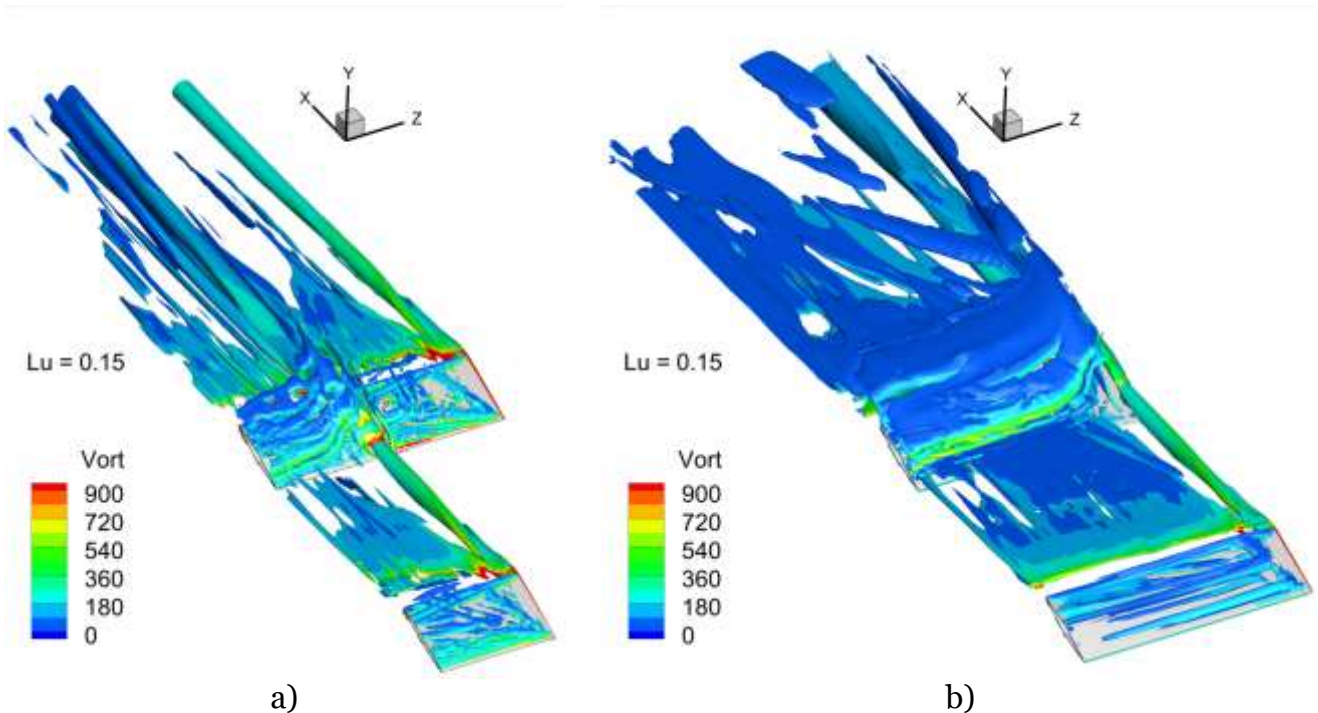
Thus, by combining various methods of identification and visualization of vortex structures, complementary results can be obtained, which is illustrated in this paper.

As mentioned above, the main vortex structures that are formed during the flow around the wing are the tip vortex, as well as the vortex sheet. In Fig. 4, with the used value of  $\tilde{\Omega}_R = 0.52$ , the main tip vortices as well as the secondary vortices are clearly distinguishable.

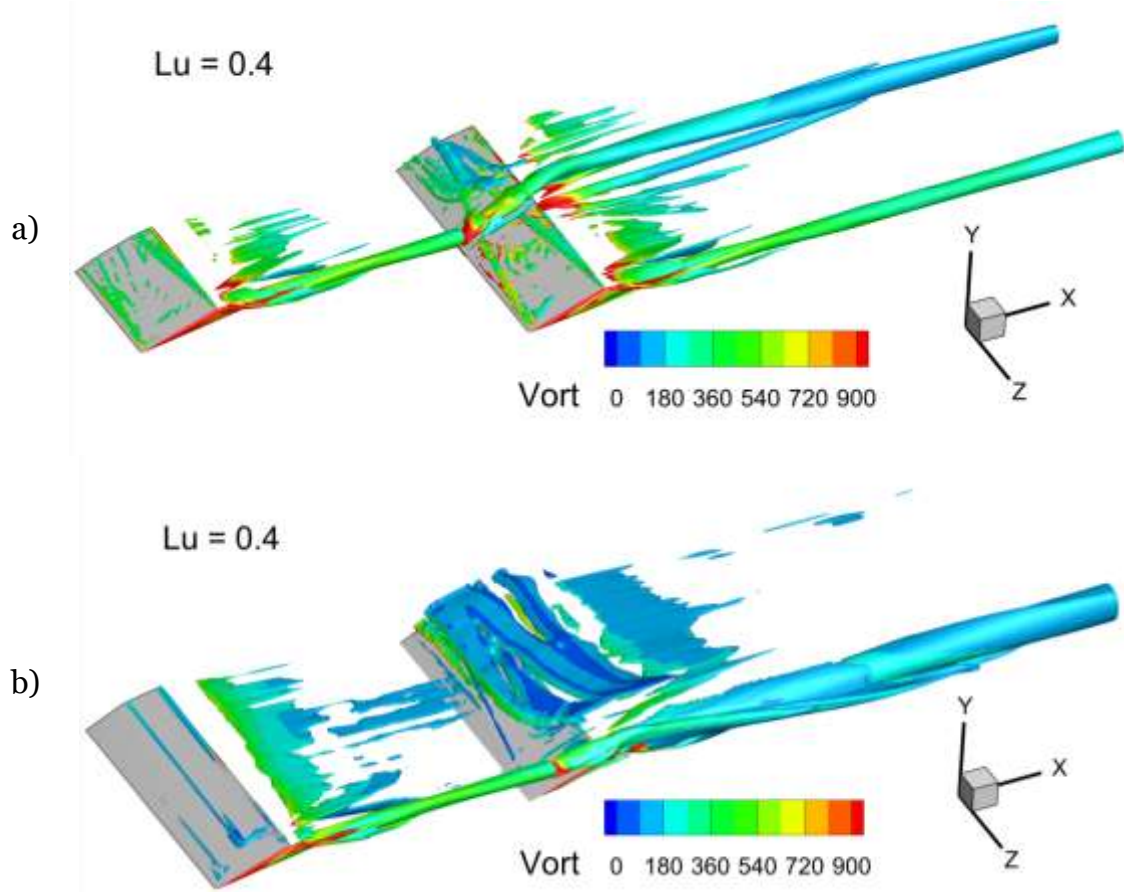
However, Figure 3 does not show the vortex sheet behind the wings, which is also an important component affecting the flow around the main wing. To display the vortex sheet, it is necessary to reduce the value of the parameter  $\tilde{\Omega}_R$  in our case.

Figure 5 shows the visualization of the flow using the Liutex criterion at the value of the parameter  $\tilde{\Omega}_R = 0.15$ . The vortex sheet is clearly visible, but the remaining vortex structures of the flow (tip and secondary vortices) become almost indistinguishable, which is especially noticeable for a configuration with a long generator.

Thus, it is necessary to adapt the values of the visualization criteria parameters used for the configurations under consideration. Figure 6 shows the visualization at the value of the Liutex parameter of the criterion  $\tilde{\Omega}_R = 0.4$  for the considered configurations with a short (a) and long (b) generator. In this figure, all the vortex structures behind the wing are clearly distinguishable: both the tip vortices and the vortex sheet. Both of these structures interact with the main wing, affecting its aerodynamic characteristics.



**Figure 5:** Visualization of vortex structures using both the Liutex criterion and the vorticity: isosurface  $\tilde{\Omega}_R = 0.15$  with values of vorticity (*Vort*) on it, for configurations with a short generator (a) and a long one (b)



**Figure 6:** Visualization of vortex structures using both the Liutex criterion and the vorticity: isosurface  $\tilde{\Omega}_R = 0.4$  with values of vorticity ( $Vort$ ) on it, for configurations with a short generator (a) and a long one (b)

The tip vortex from the short generator in the considered configuration falls on the windward side of the main wing, where it interacts with its surface (Fig. 4a – 6 a). During this interaction, secondary vortices are formed, some of which have a rotation direction that is opposite to the rotation direction of the tip vortex. The fact of the formation of secondary vortices is in qualitative agreement with experimental and numerical data for incompressible flows [26, 27].

The tip vortex from the long generator in the appropriate configuration does not fall on the surface of the main wing, but into the zone of its tip chord (Fig. 4 b – 6 b). A peculiar winding of one tip vortex onto the other occurs, followed by their unification into one longitudinal vortex structure with a larger width.

For the problem of considerate type, the longitudinal vorticity  $XVort$  can additionally be used, which makes it possible to determine and obtain a vivid visualization of the rotation direction of vortex structures, including secondary vortices. If we apply positive and negative values of  $XVort$  to the isosurface of the Liutex criterion, we get the result presented below (Fig. 7), which effectively displays the rotation direction of vortices in three-dimensional space. In Fig. 7, the red color indicates the rotation direction of the tip vortices, and the blue color indicates the opposite direction of rotation. Understanding the rotation direction of vortex structures is important, because ultimately, the effect of vortices on objects located downstream depends to a large extent, including on the direction of their rotation.

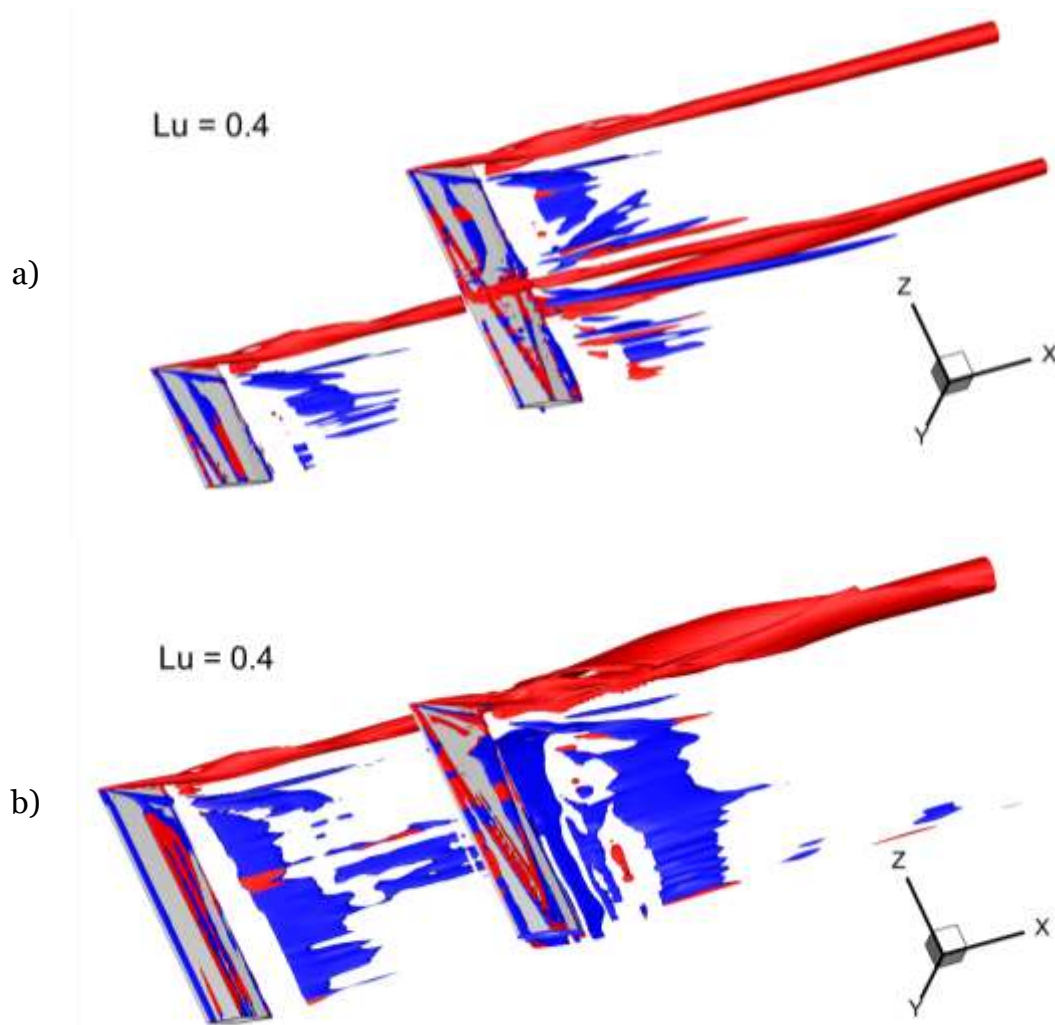


**Figure 7:** Visualization of vortex structures using both the Liutex criterion and the vorticity: isosurface  $\tilde{\Omega}_R = 0.4$  the designation of the rotation direction of the vortices, for configurations with a short generator (a) and a long one (b)

## 6. Conclusion

The paper presents the results of the analysis and scientific visualization of the problem of the vortex structures influence on the supersonic flow around a wing located at an attack angle. The dependence on the wingspan of the vortex structure generator is considered. The Mach number of the incoming flow was  $M_\infty = 3$ . Numerical simulations were performed using the author's ARES software package for parallel computing on the hybrid supercomputer system K-60 at the Keldysh Institute of Applied Mathematics RAS.

The Liutex criterion, which belongs to the third generation of such criteria, was mainly used to identify and visualize vortex structures. A combination of this method with some others was also used.

For the configuration with a short generator, it was found that the tip vortex hits on the windward surface of the main wing. Upon the interaction of the tip vortex with the wing surface several secondary vortices are formed, some of which have a rotation direction opposite to the rotation direction of the tip vortex. The form of this interaction is in qualitative agreement with experimental and numerical data for incompressible flows.

For a configuration with a long generator, another type of interaction is obtained, in which the tip vortex from the generator wing is "swirls" to the tip vortex from the main wing, followed by their merging into one longitudinal vortex structure.



The paper shows that the combination of different methods of vortex structures identification and visualization allows us to obtain complementary results. And it is the combination of different methods that makes it possible to obtain the most complete results of the analysis of flow data. This is especially true for complex turbulent flows with a large amount of data.

## References

1. Yang Wen-Jei. Handbook of flow visualization. CRC Press; 2nd edition. 2001. 724 p. ISBN 9781560324171
2. Volkov K.N. Visualization methods of vortical flows in computational fluid dynamics and their applications. Scientific and Technical Journal of Information Technologies, Mechanics and Optics, 91 3, 2014 (in Russian).
3. Epps B.P. Review of Vortex Identification Methods // 55<sup>th</sup> AIAA Aerospace Sciences Meeting. 2017. AIAA 2017-0989. DOI: 10.2514/6.2017-0989
4. Hansen C.D., Johnson C.R. (Editors). The Visualization Handbook. Academic Press. 2005. 962 p. ISBN 978-0-12-387582-2
5. Dong Y., Yan Y., Liu C. New visualization method for vortex structure in turbulence by  $\lambda_2$  and vortex filaments // Applied Mathematical Modelling, 40 1, pp. 500-509, 2016. DOI: 10.1016/j.apm.2015.04.059
6. Chen H., Wang Z., Zhu L., Wang J. Evaluation of vortex identification methods based on two- and three-dimensional swirling strengths // Physics of Fluids 30, 125102, 2018. DOI: 10.1063/1.5052309
7. Canivete Cuissa J. R., Steiner O. Innovative and automated method for vortex identification // A&A, 668, A118, 16 p., 2022. DOI: 10.1051/0004-6361/202243740
8. Xu Z., Maria A., Chelli K., Premare T. D. D., Bilbao X., Petit C., Zoumboulis-Airey R., Moulitsas I., Teschner T., Asif S., Li J. Vortex and Core Detection using Computer Vision and Machine Learning Methods // European Journal of Computational Mechanics, 32 (05), pp. 467-494, 2023. DOI: 10.13052/ejcm2642-2085.3252
9. Liu C., Gao Y., Dong X., Wang Y., Liu J., Zhang Y., Cai X., Gui N. / Third generation of vortex identification methods: Omega and Liutex/Rortex based systems // J. Hydrodyn., 31 2, pp. 205-223, 2019.
10. Liu C., Gao Y., Tian S., Dong X. Rortex—A new vortex vector definition and vorticity tensor and vector decompositions // Phys. Fluids. 30:035103, 2018.
11. Shrestha P., Nottage C., Yu Y., Alvarez O., Liu C. Stretching and shearing contamination analysis for Liutex and other vortex identification methods // Advances in Aerodynamics, 3 8, 2021.
12. Liu J., Liu C. Modified normalized Rortex/vortex identification method // Phys. Fluids. 31:061704, 6 p, 2019.
13. Kolář V., Šístek J. Stretching response of Rortex and other vortex-identification schemes // AIP Advances, 9, 105025, 2019. DOI: 10.1063/1.5127178
14. Gao Y., Yu Y., Liu J., Liu Ch. Explicit expressions for Rortex tensor and velocity gradient tensor decomposition // Phys. Fluids. 31:081704, 2019. DOI: 10.1063/1.5118948
15. Shrestha P., Nottage C., Yu Y. Stretching and shearing contamination analysis for Liutex and other vortex identification methods // Adv. Aerodyn., 3 (8), 20 p., 2021.
16. Allmaras S.R., Johnson F.T., Spalart P.R.. Modifications and Clarifications for the Implementation of the Spalart-Allmaras Turbulence Model // Seventh International Conference on CFD (ICCFD7), Big Island, Hawaii, 9-13 July 2012.
17. Toro E.F. Riemann Solvers and Numerical Methods for Fluid Dynamics. A Practical Introduction. Springer Dordrecht Heidelberg London New York (2009)
18. Borisov V.E., Davydov A.A., Kudryashov I.Yu., Lutsky A.E., Men'shov I.S. Parallel Implementation of an Implicit Scheme Based on the LU-SGS Method for 3D Turbulent Flows // Mathematical Models and Computer Simulations, 7 (3), p. 222-232, 2015.

19. Borisov V.E., Davydov A.A., Kydryshov I.Yu., Lutsky A.E. ARES software package for numerical simulation of three-dimensional turbulent flows of viscous compressible gas on high-performance computing systems, Certificate of registration of a computer program RU 2019667338, (23 December 2019) (in Russian).
20. Supercomputer system K-60 // <https://www.kiam.ru/MVS/resourses/k60.html> .
21. Jeong J., Hussain F. On the identification of a vortex // *Journal of Fluid Mechanics*, V. 285, pp. 69–94, 1995.
22. Hunt J.C.R., Wray A.A., Moin P. Eddies, stream, and convergence zones in turbulent flows // Technical Report N<sup>o</sup> CTR-S88. Palo Alto: Center for Turbulent Research. pp 193–208, 1988.
23. Konstantinovskaya T.V., Borisov V.E. , Lutsky A.E. Visualization Problems of a Supersonic Tip Vortex in a Heat Wake // *Scientific Visualization*, 14 4, pp. 71 – 82, 2022. DOI: 10.26583/sv.14.4.07
24. Chen C., Wang Z., Gursul I. Experiments on tip vortices interacting with downstream wings // *Experiments in Fluids*. 2018. 59 5. Art. 82. 24 p. DOI: 10.1007/s00348-018-2539-7
25. Strawn & Kenwright 1999 et al R.C. Strawn, D.N. Kenwright, J. Ahmad, Computer visualization of vortex wake systems, *AIAA Journal* (1999), volume 37(4), pp. 511–512.
26. Gadzhiev D.A., Gaifullin A.M. Evolution of Two Vortices Near a Solid Surface // *J. Appl. Mech. Tech. Phys.*, 59:2, pp 212–218, 2018.